

Stress-driven migration of symmetrical $\langle 100 \rangle$ tilt grain boundaries in Al bicrystals

Tatiana Gorkaya, Dmitri A. Molodov*, Günter Gottstein

Institute of Physical Metallurgy and Metal Physics, RWTH Aachen University, D-52056 Aachen, Germany

Received 3 July 2009; accepted 20 July 2009

Available online 18 August 2009

Abstract

Stress-induced migration of planar grain boundaries in aluminum bicrystals was measured for both low- and high-angle symmetrical $\langle 100 \rangle$ tilt grain boundaries across the entire misorientation range ($0\text{--}90^\circ$). Boundary migration under a shear stress was observed to be coupled to a lateral translation of the grains. Boundaries with misorientations smaller than 31° and larger than 36° moved in opposite directions under the same applied external stress. The measured ratios of the normal boundary motion to the lateral displacement of grains are in an excellent agreement with theoretical predictions. The coupled boundary motion was measured in the temperature range between 280 and 400°C , and the corresponding activation parameters were determined. The results revealed that for mechanically induced grain-boundary motion there is a misorientation dependence of migration activation parameters. The obtained results are discussed with respect of the mechanism of grain-boundary motion.

© 2009 Acta Materialia Inc. Published by Elsevier Ltd. All rights reserved.

Keywords: Boundary motion; Shear strain; Coupling; Dislocations

1. Introduction

Motion of symmetrical low-angle tilt grain boundaries under a mechanical stress was predicted by Read and Shockley [1] and first experimentally observed in the classical experiments by Washburn and Parker [2], Li et al. [3] and Bainbridge et al. [4] in the 1950s for low-angle boundaries in Zn. The mechanism of this motion is the collective glide of edge dislocations which comprise such boundaries [1]. Shear stress acting on the boundary plane causes a glide force on each edge dislocation [5], and thus results in the motion of the entire boundary. The dislocation glide causes a shear strain of the crystal region through which the boundary has migrated.

In a previous paper [6], we reported the results of experiments with symmetrical low-angle $\langle 100 \rangle$ tilt boundaries in Al bicrystals. The dependence of the normal boundary velocity on the driving force was measured, and the

magnitude of the boundary mobility was determined. According to the edge dislocation structure of such boundaries, their normal displacement under a mechanical stress was confirmed to be coupled to a shear deformation, which in a bicrystal with a planar boundary is observed as a tangential translation of the adjoining grains. In similarly loaded bicrystals, $\langle 100 \rangle$ tilt boundaries with misorientation angles close to 0° and close to 90° were observed to move in opposite directions. This demonstrated that low-angle $\langle 100 \rangle$ boundaries with tilt angles from opposite sides of the misorientation range ($0\text{--}90^\circ$), which consist of different dislocation arrangements, react with a different response to an applied mechanical stress [6].

The dislocation glide mechanism of boundary motion coupled to a shear deformation is commonly understood to be limited to boundaries with low tilt angles, since at higher misorientations the dislocation model is no longer applicable. However, recent theoretical investigations by Cahn et al. [7–9] and by Caillard et al. [10] predict that a coupling between normal boundary motion and lateral translation of the adjacent grains can occur for high-angle

* Corresponding author. Tel.: +49 2418026873; fax: +49 2418022301.
E-mail address: molodov@imm.rwth-aachen.de (D.A. Molodov).

boundaries as well, and this has been also corroborated by molecular dynamics (MD) computer simulations by Mishin et al. [11,12], Zhang et al. [13] and Elsener et al. [14]. In fact, Watanabe et al. [15] and Fukutomi et al. [16–18] reported that some high-angle tilt boundaries with low Σ CSL orientation relationships in Zn and Al bicrystals can be moved by an applied shear stress in this fashion, which causes a shape change of the bicrystal. A similar behavior was observed by Sheikh-Ali et al. [19–21] for various low Σ tilt boundaries in Zn and by Yoshida et al. [22] for a $\Sigma 11$ boundary in cubic ZrO_2 bicrystals. The motion of various low- and high-angle grain boundaries under an applied shear stress in Al was also reported by Winning et al. [23–25]. Quite recently, the coupling between grain-boundary motion and shear deformation was observed by Mompou et al. in in situ TEM experiments in Al polycrystals [26].

In recent years grain-boundary migration coupled to grain translation has become a subject of extensive discussion in the literature with respect to the impact of this phenomenon on mechanical properties of ultra-fine-grained and nanocrystalline materials. As revealed by molecular dynamics (MD) simulations, probably due to constraints of both nucleation and motion of dislocations in very small grain-sized polycrystals, there is a critical grain size, below which even a reversed Hall–Petch effect can be observed (flow stress decreases with decreasing grain size), i.e. the mechanism of plasticity is probably changed [27,28]. Grain-boundary migration accompanied by shear is considered as one of the alternative deformation mechanisms of nanocrystalline materials [29,30]. In fact, recent TEM investigations of stress-assisted grain growth [31] and boundary motion associated with shape changes [32] in nanocrystalline aluminum films provide evidence that plasticity can effectively be mediated by grain-boundary migration.

However, there is an obvious lack of reliable experimental data on boundary migration–shear coupling, and in situ TEM observations on polycrystals only are insufficient for a comprehensive understanding of this phenomenon. Theoretical models and results of computer simulations are most appropriately validated in experiments on individual grain boundaries with well-defined structure, i.e. in specially grown bicrystals. Moreover, measurements of boundary migration coupled to shear under a constant mechanical loading provide the opportunity to extract the value of boundary mobility, to determine its temperature dependence and to compare the migration kinetics of structurally different grain boundaries.

In the current paper we apply this approach for an investigation of boundary migration coupled to shear in bicrystals containing various low and high-angle $\langle 100 \rangle$ tilt boundaries.

2. Experimental

The experiments were conducted on commercially pure aluminum (99.998%) bicrystals, grown in a graphite mold

by the Bridgman method. Symmetrical low- and high-angle $\langle 100 \rangle$ tilt grain boundaries with misorientation angles across the entire misorientation range between 0° and 90° were examined. The orientation of the crystallographic axes of the monocrystal seeds and the fabricated bicrystals was measured by the Laue technique [1] with an accuracy of $\pm 0.2^\circ$. The measured misorientations across the boundary and the misalignment of the normal directions to an ideal $[001]$ axis for both adjoining crystals in the investigated bicrystals (Fig. 1) are given in Table 1.

Shear stress-induced boundary motion was measured in the specimens with a cross-section of about $4.9 \text{ mm} \times 4.7 \text{ mm}$ (Fig. 1b) fabricated from the grown bicrystals by electro-discharge machining and subjected to tensile loading as depicted in Fig. 2. Constant tensile forces between 5 and 20 N resulted in shear stresses in the range between 0.05 and 0.5 MPa. The experiments were conducted in the temperature interval between 280 and 400°C , and the temperature was controlled with an accuracy of 0.5° . Prior to annealing under stress the specimens were electrolytically polished. The annealing time under stress ranged from 0.9×10^3 to 14.4×10^3 s (15 and 240 min). The boundary displacement was revealed and measured by optical orientation contrast on the surface of the bicrystal (Fig. 3).

In order to determine the direction of boundary motion the specimens were etched after annealing under stress in a solution of 18 ml HCl, 7 ml HNO_3 , and 3 ml HF for 3–4 s. Due to different orientations of the square-shaped etch pits on the (100) surface the final boundary location and, therefore, the direction of boundary migration was identified (Fig. 3).

For characterization of the relation between the lateral translations of the grains parallel to the boundary and the normal boundary displacement the surface of the

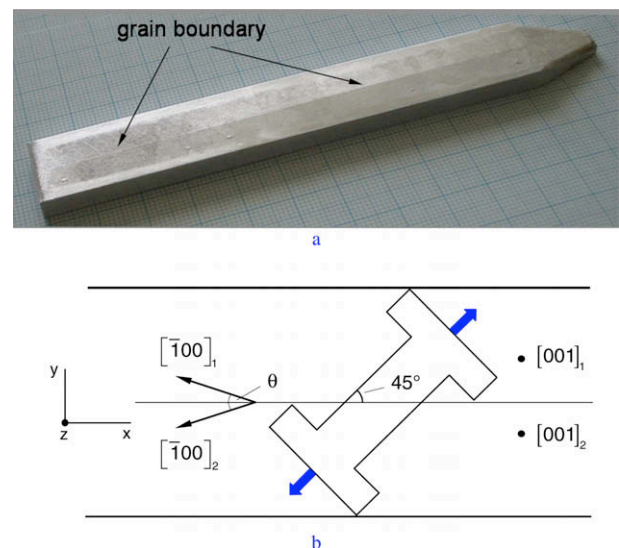


Fig. 1. (a) Grown Al bicrystal with a slightly etched surface to reveal the grain boundary and (b) specimens (with cross-sections $\sim 4.9 \text{ mm} \times 4.7 \text{ mm}$) for the tensile loading.

Table 1

Misorientations θ and orientations of adjoining crystals in the investigated bicrystals; Δx and Δy are deviations of the $[0\ 0\ 1]$ direction from the sheet normal, Δz is the rotation angle around the z axis (Fig. 1b), i.e. $\theta = |\Delta z_1| + |\Delta z_2|$.

$\theta \pm 0.5$ (°)	Crystal 1			Crystal 2		
	Δx (°)	Δy (°)	Δz (°)	Δx (°)	Δy (°)	Δz (°)
5.6	-1.2	-0.2	2.8	0.6	-0.3	-2.8
5.7	-0.7	-0.3	3.1	0.2	-0.2	-2.6
5.8	-0.3	-0.2	3.2	0.2	-0.2	-2.6
6.8	0.3	-0.8	-2.9	-0.9	-0.7	3.9
7.3	0.1	-0.8	-3.2	-0.2	-0.7	4.1
10.2	-0.5	-0.9	4.1	0.4	-0.5	-6.1
10.5	0.2	0.5	4.6	-0.4	0.2	-5.9
17.6	-0.5	-0.5	9.0	-0.5	-0.5	-8.6
17.7	0.3	-0.4	9.0	0.4	-0.3	-8.7
17.8	0.4	-0.4	9.0	0.5	-0.4	-8.8
21.5	0.5	1.5	-9.9	0.9	-1.0	11.6
22.0	0.1	0.6	-10.7	1.0	-1.0	11.3
28.9	-0.1	-1.1	-14.2	0.2	-0.7	14.7
29.2	0.0	-0.7	-14.3	0.4	-0.9	14.9
30.5	0.3	-0.9	-14.2	0.4	-1.0	16.3
36.5	0.2	0.3	18.8	0.5	-0.5	-17.7
37.5	-1.1	-2.9	19.7	-1.0	-1.2	-17.8
43.7	0.6	1.3	-22.0	0.0	0.1	21.7
45.4	0.3	0.5	-22.1	0.3	-0.1	23.3
48.9	0.2	-0.1	24.9	-0.3	0.1	-24.0
49.0	0.2	0.2	24.7	-0.7	0.2	-24.3
55.4	0.0	-0.1	28.3	0.2	0.3	-27.1
56.2	-0.7	-0.8	28.5	2.7	-1.8	-27.7
60.0	0.0	0.0	30.0	0.2	-0.1	-30.0
61.0	-0.1	-0.2	30.3	-0.2	-0.9	-30.7
66.6 ₁	-0.2	-0.6	33.3	0.8	-0.4	-33.3
66.6 ₂	-0.9	-0.5	33.4	1.2	-0.6	-33.2
67.5	0.6	-0.6	33.9	0.2	-0.5	-33.6
76.1	-0.9	-0.5	38.3	0.0	-0.5	-37.8
76.3	-0.9	-0.5	38.6	-0.2	-0.4	-37.7
81.0	-0.6	0.5	40.7	-1.1	-0.2	-40.3
81.2	-0.5	0.1	40.5	-0.5	-0.1	-40.7
84.2	-0.4	0.5	-42.4	-1.0	-0.6	41.8
84.4	0.2	-0.6	-42.3	0.7	0.5	42.1

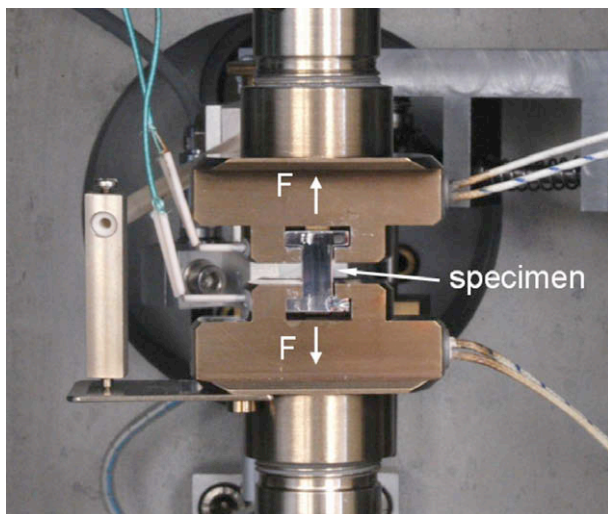


Fig. 2. The specimen is heated through both the top and bottom grips of the testing machine and subjected to constant tensile force after the specimen reached the desired temperature.

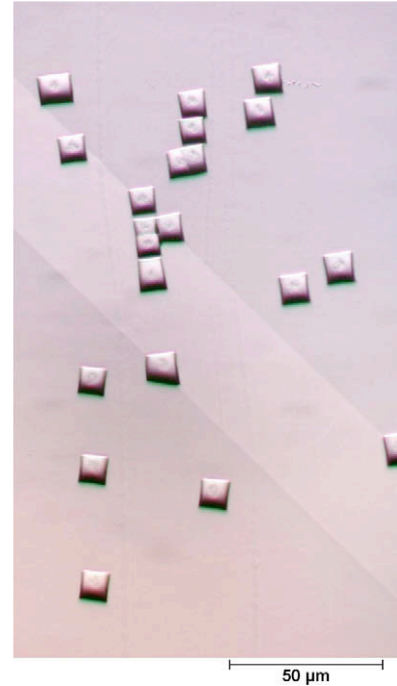


Fig. 3. Traces of the initial and final position of a 76.1° $\langle 100 \rangle$ tilt boundary on the specimen surface after 75 min annealing at 320°C under an applied tensile stress of 0.43 MPa . Square-shaped etch pits on the surface of the consumed and the growing grain are oriented differently and therefore reveal the direction of boundary migration (right to left).

specimens was scratched parallel to their axis prior to annealing to produce reference marks (Fig. 4).

3. Results

The results revealed that mechanically induced boundary migration associated with a shear deformation was not restricted to symmetrical low-angle and some special low Σ CSL boundaries but occurred for all investigated high-angle $\langle 100 \rangle$ tilt boundaries. Fig. 4 depicts the surface of bicrystals with 17.8° and 66.6° $\langle 100 \rangle$ tilt boundaries after annealing under stress. As apparent from the marking lines on the surface of the bicrystals and the shape change of the specimens (Fig. 4b), the normal boundary displacement is accompanied by shearing of the specimen region through which the boundary has migrated.

The experiments showed that in similarly loaded bicrystals, $\langle 100 \rangle$ tilt boundaries with $\theta < 31^\circ$ and $\theta > 36^\circ$ move in opposite directions.

Furthermore, the experiments revealed that boundary migration under an applied mechanical stress was thermally activated and that its rate v_n depended on temperature according to an Arrhenius-type dependence

$$v_n = v_0 \exp(-H/kT) \quad (1)$$

where H is the activation enthalpy of grain boundary migration.

The grain boundary mobility m in the current experiments was determined from the relation between the normal boundary velocity v_n and the driving force p :

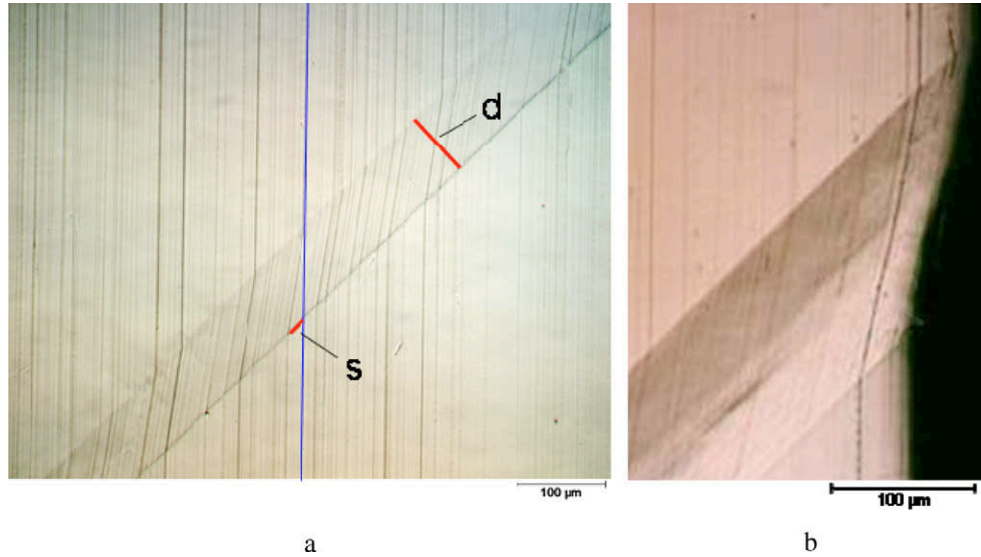


Fig. 4. Grain boundary migration accompanied by shear for (a) 17.8° $\langle 100 \rangle$ symmetrical tilt boundary after 68 min annealing at 375°C under a tensile stress of 0.27 MPa , and (b) 66.6° $\langle 100 \rangle$ symmetrical tilt boundary after 170 min annealing at 355°C under a tensile stress of 0.26 MPa . The coupling factor β was determined as the ratio of the grain's lateral translation s to the normal boundary displacement d .

$$m = v_n/p \quad (2)$$

The driving force on a symmetrical tilt boundary with misorientation angle θ caused by a shear stress τ reads

$$p = \tau \sin \varphi \quad (3)$$

where $\varphi = \theta$ for misorientations close to 0 , and $\varphi = \theta - 90^\circ$ for θ close to 90° . Eq. (3) derived for low-angle boundaries [1] was assumed to hold also for high-angle boundaries.

Since the driving force is independent of temperature, the temperature dependence of v_n is the temperature dependence of the grain boundary mobility

$$m = v_n/p = m_0 \exp(-H/kT) \quad (4)$$

The boundary motion was measured in the temperature range between 280 and 400°C (Fig. 5). The migration activation parameters (H and m_0) obtained from Arrhenius plots for all investigated boundaries are listed in Table 2.

Boundary migration coupled to a shear was not the only possible response of the boundary to the applied stress observed in the current experiments. In bicrystals with high-angle boundaries a rigid translation of grains along the boundary plane (grain boundary sliding) occurred, especially in the high-temperature regime (Fig. 6). Investigations into the details of this phenomenon (threshold stress, temperature range, etc.) in Al bicrystals containing different symmetrical tilt grain boundaries are in progress.

4. Discussion

4.1. Coupling normal grain boundary motion to shear strain

The experiments have unambiguously shown that not only low-angle tilt boundaries produce a shear during their motion under stress [1–4,6], but also high-angle boundary migration is accompanied by a shear deformation of the

crystal region swept by the boundary. Evidently the motion in this fashion is a typical response of any symmetrical $\langle 100 \rangle$ tilt boundary, not only some low Σ boundaries [15–22], to the applied shear stress.

As suggested by Cahn and Taylor [7], a coupling between boundary migration normal to its plane and the lateral translation of grains can be described by the ratio $\beta = v_{\parallel}/v_n = s/d$ (Fig. 4a), where v_{\parallel} and v_n are the lateral translation rate and the boundary velocity, respectively. The ratio β is referred to as the coupling factor.

The experimentally obtained values of the coupling factor, averaged over all investigated specimens of a respective bicrystal, are given in Fig. 7. Since boundaries with $\theta < 31^\circ$ and $\theta > 36^\circ$ migrate in opposite directions, the corresponding values of β are different in sign.

A misorientation dependence of the coupling factor for low-angle symmetrical tilt boundaries was predicted by Read and Shockley. For a symmetrical tilt boundaries moving by collective glide of their structural dislocations elementary dislocation geometry requires that the coupling factor β relates to the misorientation angle θ as $\beta = 2 \tan(\theta/2) \approx \theta$ [1]. As has been established by computer simulations [10] and demonstrated experimentally [6], for low-angle $\langle 100 \rangle$ tilt boundaries there are two branches of the misorientation dependence of β . For misorientations θ close to 0 , i.e. when boundary motion can formally be represented by slip of dislocations with $\mathbf{b} = a \langle 010 \rangle$ on $\{001\}$

$$\beta_{\langle 010 \rangle} = 2 \tan\left(\frac{\theta}{2}\right) \quad (5)$$

whereas for θ close to 90° (slip on $\{110\}$ with $\mathbf{b} = \frac{a}{2} \langle 110 \rangle$)

$$\beta_{\langle 110 \rangle} = -2 \tan\left(\frac{\pi}{4} - \frac{\theta}{2}\right) \quad (6)$$

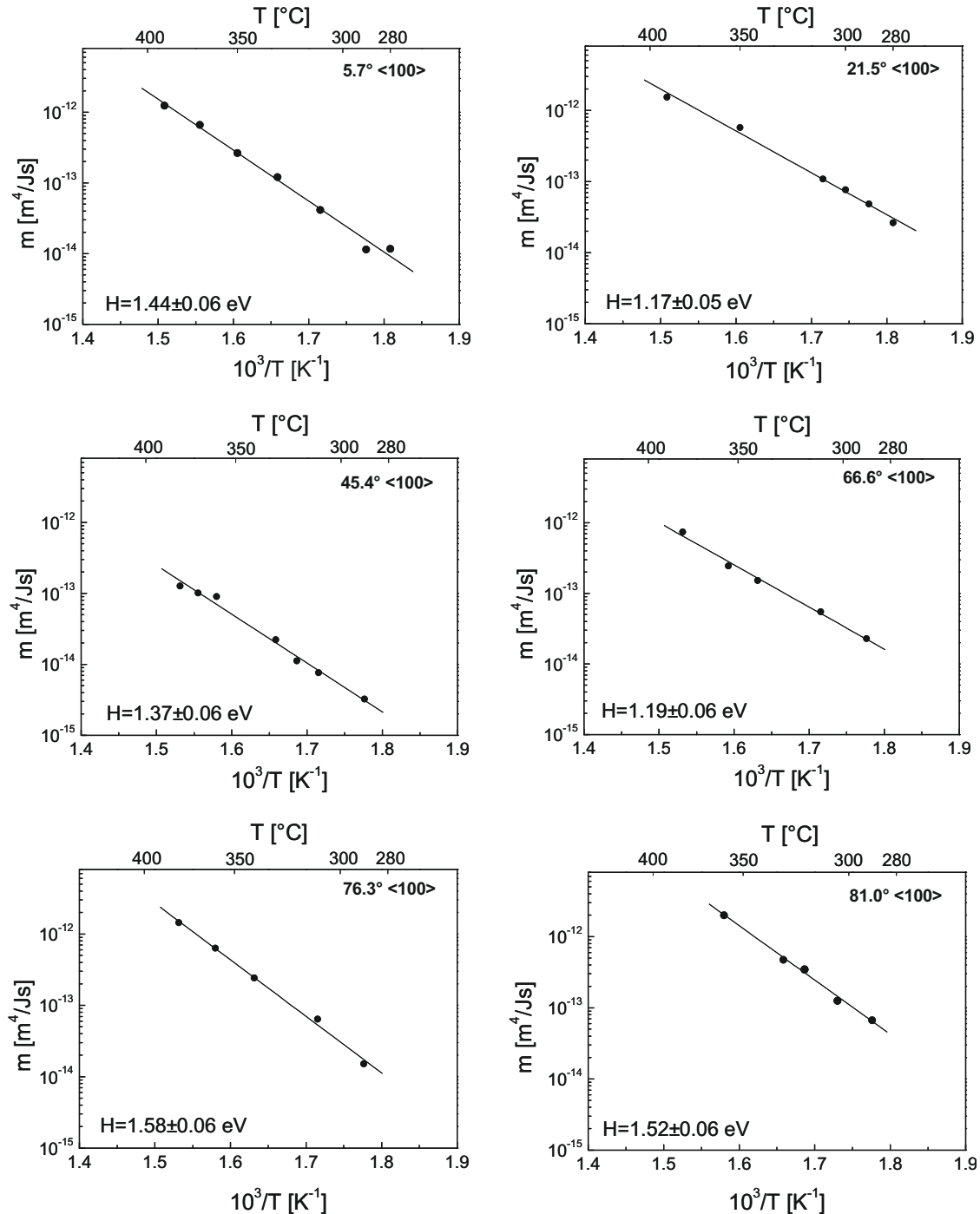


Fig. 5. Temperature dependence of the mobility for some investigated stress-driven $\langle 100 \rangle$ tilt grain boundaries.

Recently, Cahn et al. [8] have analyzed the Frank–Bilby equation [33] for the dislocation content of grain boundaries. Two solutions of this equation for $\langle 100 \rangle$ symmetrical boundaries between fcc crystals were examined, each of which is an accurate description for the two types of low-angle grain boundaries that exist at the extremes of the misorientation range between 0° and 90° . The model of coupled boundary motion by Cahn et al. [8,9], based on

this analysis, predicts that Eqs. (5) and (6), derived for low-angle boundaries, retain their validity also in the high-angle regime.

As seen in Fig. 7, there is excellent agreement between the current experimental data and the coupling factors calculated according to Eqs. (5) and (6). Therefore, the experimental results evidence that for $\langle 100 \rangle$ tilt boundaries there are indeed two geometrically different mechanisms

Table 2
Migration activation enthalpy and pre-exponential mobility factor for the motion of $\langle 100 \rangle$ tilt boundaries in Al coupled to shear strain.

Tilt angle, θ ($^\circ$)	Activation enthalpy, H (eV)	Pre-exponential factor, $\log(m_0)$ ($\text{m}^4 \text{J}^{-1} \text{s}^{-1}$)
5.6	1.47 ± 0.37	0.07 ± 3.09
5.7	1.44 ± 0.06	-1.01 ± 0.49
5.8	1.36 ± 0.10	-1.46 ± 0.81
6.8	1.38 ± 0.10	-0.86 ± 0.81
7.3	1.52 ± 0.10	0.29 ± 0.79
10.2	1.37 ± 0.39	-0.90 ± 3.30
10.5	1.42 ± 0.33	-0.53 ± 2.74
17.6	1.36 ± 0.40	-1.63 ± 3.39
17.7	1.35 ± 0.25	-1.76 ± 2.04
17.8	1.44 ± 0.24	-1.01 ± 1.97
21.5	1.17 ± 0.05	-2.87 ± 0.41
22.0	1.32 ± 0.30	-1.67 ± 2.44
28.9	1.12 ± 0.10	-4.14 ± 0.81
29.2	1.36 ± 0.16	-2.45 ± 1.30
30.5	1.32 ± 0.20	-2.82 ± 1.68
36.5	1.10 ± 0.14	-4.71 ± 1.17
37.5	1.51 ± 0.12	-1.37 ± 0.93
43.7	1.13 ± 0.06	-4.35 ± 0.50
45.4	1.37 ± 0.06	-2.28 ± 0.52
48.9	1.41 ± 0.26	-1.79 ± 2.17
49.0	1.35 ± 0.12	-2.35 ± 1.01
55.4	0.91 ± 0.09	-5.71 ± 0.78
56.2	0.97 ± 0.06	-4.88 ± 0.51
60.0	1.65 ± 0.36	0.45 ± 2.95
61.0	1.46 ± 0.11	-1.17 ± 0.88
66.6	1.20 ± 0.26	-3.44 ± 2.14
66.6	1.19 ± 0.06	-3.03 ± 0.47
67.5	1.25 ± 0.22	-2.90 ± 1.75
76.1	1.58 ± 0.09	0.48 ± 0.70
76.3	1.58 ± 0.06	0.31 ± 0.51
81.0	1.52 ± 0.06	0.34 ± 0.55
81.2	1.44 ± 0.09	-0.32 ± 0.78
84.4	1.40 ± 0.13	-0.22 ± 1.08
84.2	1.50 ± 0.05	0.72 ± 0.39

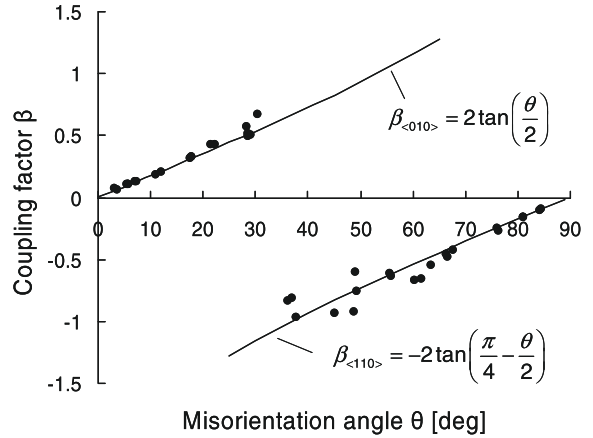


Fig. 7. Misorientation dependence of measured (points) and calculated (lines) coupling factors for the investigated $\langle 100 \rangle$ symmetrical tilt grain boundaries.

($\langle 100 \rangle$) and $\langle 110 \rangle$ modes as defined by Cahn et al. [8,9]) of coupling between normal boundary motion and lateral grain translation. Furthermore, the current results substantiate that the Frank–Bilby equation still applies, although in high-angle boundaries the structural dislocations cannot be resolved.

The switching between coupling modes was observed to occur at a misorientation angle between 30.5° and 36.5° . An analysis of the critical resolved shear stress for $\langle 100 \rangle$ tilt boundary motion by considering the Peierls–Nabarro stress for individual dislocation glide revealed [8,9] that $\{110\}$ slip in the $\langle 110 \rangle$ direction responsible for the $\langle 110 \rangle$ mechanism of coupling must be much easier than $\{100\}$ slip in the $\langle 100 \rangle$ direction. Therefore, the crossover between the two operative mechanisms in the coupled

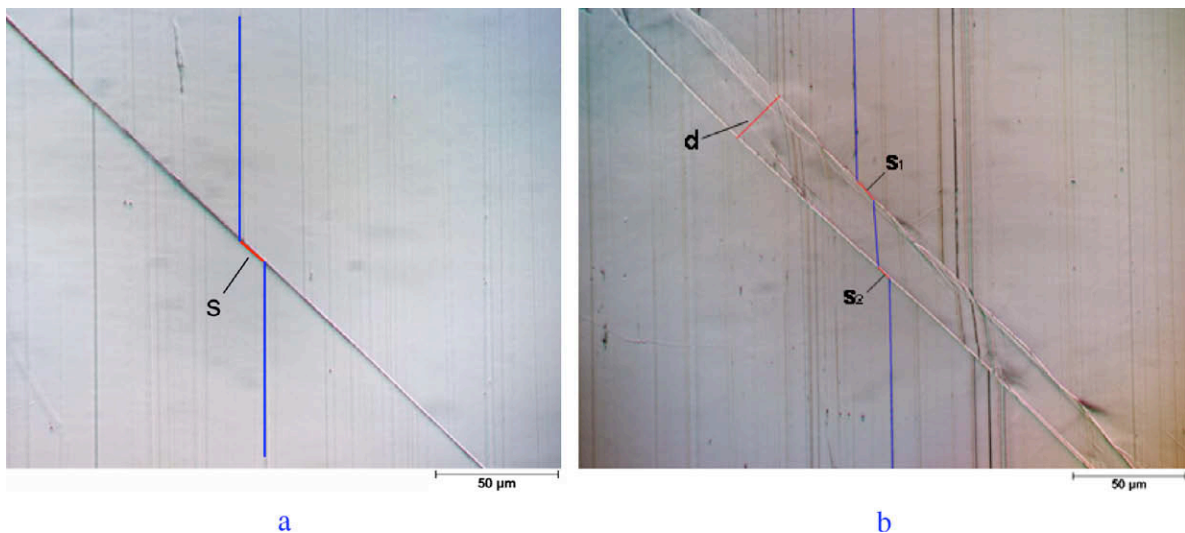


Fig. 6. (a) Sliding (s) along a 28.2° $\langle 100 \rangle$ symmetrical tilt boundary during annealing at 360°C under a tensile stress of 0.45 MPa . (b) Coupled migration of a 30.5° $\langle 100 \rangle$ symmetrical tilt boundary at 360°C under a tensile stress of 0.42 MPa , accompanied by sliding during the initial (s1) and the final (s2) stages of the annealing.

motion of $\langle 100 \rangle$ tilt boundaries can be expected at a misorientation angle $\theta < 45^\circ$ as is, in fact, observed in the current experiment. It is worth noting that although this analysis was performed by an examination of the (100) and (110) sections of gamma surfaces calculated with the embedded-atom potential for Cu [8,9], the prediction is consistent with the current result obtained on Al bicrystals.

4.2. Activation parameters of the migration of stress-driven $\langle 100 \rangle$ boundaries and their interdependence

The experiments revealed that the temperature dependence of the mobility of stress-driven symmetrical $\langle 100 \rangle$ tilt boundaries depends on misorientation angle. As depicted in Fig. 8a, the measured activation enthalpy of stress-driven boundary motion varies with misorientation angle within a rather wide range between 1.0 and 1.6 eV. However, the scatter of the activation enthalpy values is not uniform over the entire range of tilt angles. For boundaries in both low-angle regimes ($\theta < 18^\circ$ and $\theta > 76^\circ$) the migration activation enthalpy was virtually the same with an only slight scatter from the mean value of about $H = 1.45$ eV.

By contrast, in the high-angle regime the activation enthalpy changes considerably (Fig. 8a). A closer inspection of the $H(\theta)$ plot reveals, however, that there is a specific misorientation dependence of the activation enthalpy for high-angle boundaries, such that the lower H values correspond to boundaries which can be associated with misorientations close to low Σ CSL orientation relationships.

The pre-exponential mobility factor m_0 behaves similarly (Fig. 8b). In both low-angle ranges the m_0 values were about $10^{-1} \text{ m}^4 \text{ J}^{-1} \text{ s}^{-1}$, whereas in the high-angle regime they were found to be essentially different. For boundaries with low activation enthalpy the pre-exponential factor was up to five orders of magnitude smaller than for low-angle and high-angle boundaries with high activation enthalpy (Fig. 8b).

An analysis of the obtained activation enthalpy H and pre-exponential factor m_0 renders that they do not scatter stochastically, but are related. The changes of H and m_0 with misorientation angle follows the compensation law, i.e. there is a relationship between activation enthalpy and pre-exponential factor, such that the activation enthalpy changes linearly with $\ln(m_0)$ (Fig. 9a):

$$H = kT_c \ln(m_0) + B \quad (7)$$

where B is a constant and T_c is the critical (compensation) temperature, which is defined by

$$m_{T_c} = m_0 \exp(-B/kT_c) \quad (8)$$

From Fig. 9a it can be extracted that $T_c \approx 200^\circ \text{C}$. Above this temperature the boundaries with a higher activation enthalpy (measured for low-angle and non-coincidence high-angle $\langle 100 \rangle$ tilt boundaries) move faster (Fig. 9b). The migration activation enthalpy for high-angle $\langle 100 \rangle$ boundaries with tilt angles close to low Σ CSL orientations was found to be lower but also associated with a smaller pre-exponential factor. Correspondingly, these boundaries will be more mobile at temperatures below T_c .

The compensation effect was observed in various physical and physico-chemical processes, particularly in thermally activated grain boundary processes, like grain boundary migration, diffusion and internal friction [34–36]. The fundamentals of this effect are discussed elsewhere [37,38].

It is worth noting that the migration activation enthalpies of $\langle 100 \rangle$ tilt grain boundaries obtained in the current experiment differ from those obtained in experiments with curvature-driven $\langle 100 \rangle$ tilt grain boundaries in bicrystals of high-purity Al. According to different authors [39–41] the activation enthalpies for migration of curvature-driven boundaries range from 0.7 up to 2.8 eV. This difference in the migration activation enthalpy for differently driven boundaries strongly indicates that the migration mechanisms may depend on the kind of driving force for boundary motion and its coupling with the boundary structure.

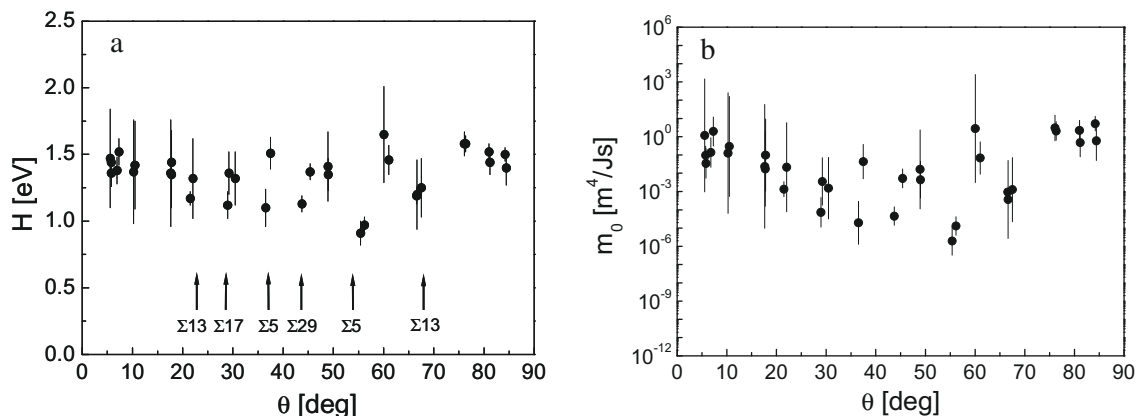


Fig. 8. Activation parameters (activation enthalpy and pre-exponential factor of mobility equation) of stress-induced migration of the investigated $\langle 100 \rangle$ symmetrical tilt grain boundaries.

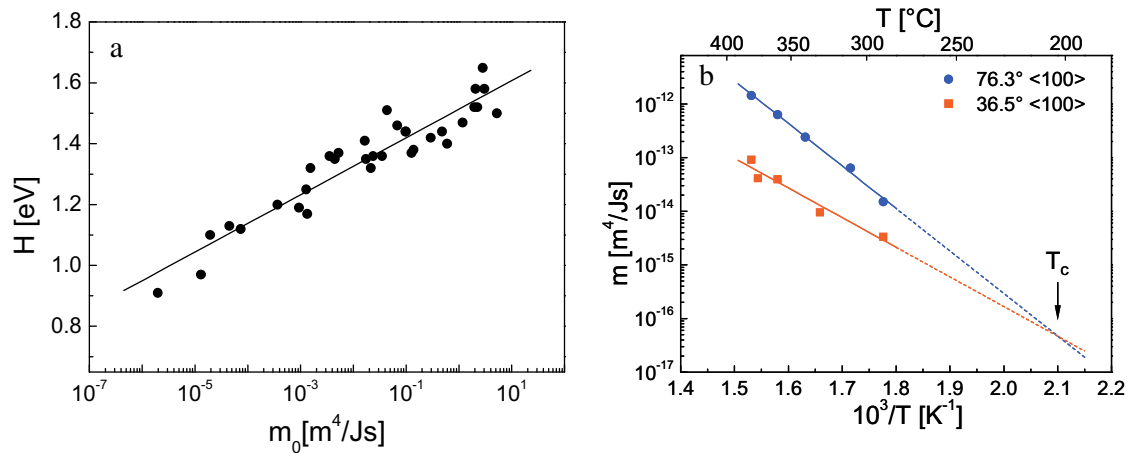


Fig. 9. (a) Relationship between activation enthalpy H and pre-exponential factor m_0 obtained for stress-driven migration of symmetrical $\langle 100 \rangle$ tilt grain boundaries and (b) mobility vs. reciprocal temperature for $76.3^\circ \langle 100 \rangle$ and $36.5^\circ \langle 100 \rangle$ boundaries.

4.3. On the mechanism of stress-driven migration of $\langle 100 \rangle$ tilt boundaries

MD simulations [9,10] suggest that there are two basic mechanisms of shear stress-induced migration of the $\langle 100 \rangle$ tilt boundaries. They correspond to boundary motion in $\langle 100 \rangle$ and $\langle 110 \rangle$ modes. The common feature of these mechanisms is that a boundary moves by conversion of atomic lattice units of one crystal into structural units of the other crystal which are differently oriented and located. Such a rearrangement includes local atomic displacements and subsequent rotation of atomic groups (atomic shuffling) that comprise the structural units of the boundary [9]. Boundary motion in the normal direction proceeds first by creation of an “island” of one crystal orientation in the neighboring crystal. Laterally this “island” is separated from the disoriented crystal by a line defect known as disconnection [42]. In response to the shear stress acting on the boundary, this defect glides on the boundary plane extending the “island”. When the disconnection loop extension is completed, the entire boundary is displaced in the normal direction by the step height of the disconnection h , and the neighboring crystals are translated by the magnitude of the disconnection Burgers vector b_d , such that $b_d = \beta \cdot h$ [9,42].

An important feature of the migration mechanism for $\langle 100 \rangle$ symmetrical tilt boundaries found in simulations is that it does not involve diffusion. The formation of an “island” of critical size, however, is a thermally activated process. The two mechanisms found in simulations of $\langle 100 \rangle$ tilt boundary motion differ with respect to the form of involved structural units and the displacement of atomic sites [9]. However, irrespective of the mode of coupling, in both low-angle regimes the experimentally obtained migration activation enthalpy is essentially the same. Furthermore, within the angular ranges where coupled boundary motion occurs in the same mode (up to 30.5° and above 36.5°) the activation parameters do not remain constant.

Evidently, the activation parameters H and m_0 are not defined by the geometrical mode of boundary motion, $\langle 100 \rangle$ or $\langle 110 \rangle$, rather than by the boundary structure as defined by the tilt angle θ . The more ordered the structure of the boundaries as denoted by low Σ orientations the lower the activation parameters for their motion under the applied stress.

The measured activation enthalpy for coupled boundary motion in both low-angle regimes amounts to about 1.45 eV, which is very close to the activation enthalpy of bulk self diffusion in Al ($H_{sd} = 1.47$ eV [43]). This suggests that the elementary step of boundary motion is associated with a bulk diffusion process, e.g. a displacement of dislocations of other character and Burgers vectors than the geometrically necessary dislocations responsible for the tilt θ . Such dislocations compensate deviations from the perfect tilt disorientation between adjacent crystals in real bicrystals. In order to maintain the given boundary geometry these dislocations must displace with the moving boundary, which requires climb controlled by bulk diffusion [18,44,45].

The current experimental results, however, do not comply with this interpretation. First, if boundary motion is controlled by dislocation climb, the rate of boundary migration (or dislocation drag) should depend on the number of the dislocations which have to climb – the higher the density of such dislocations the lower the boundary migration rate. Among the bicrystals investigated in the current experiments there were two sets of samples with the same angle of rotation around the $[001]$ axis (tilt angle) $\theta = 66.6^\circ$ but different “second tilt” component ξ that is defined as $\xi = |\Delta x_1| + |\Delta x_2|$ (Fig. 1) and amounts to $\xi_{66.6(1)} = 1.0^\circ$ and $\xi_{66.6(2)} = 2.1^\circ$ (Table 1). Correspondingly, the density of the respective dislocations in the first bicrystal set is lower by at least a factor of 2 than that in the second set. Therefore, a boundary in the 66.6(1) bicrystal is expected to move faster than a boundary in the 66.6(2) bicrystal. As seen in Fig. 10, however, the opposite

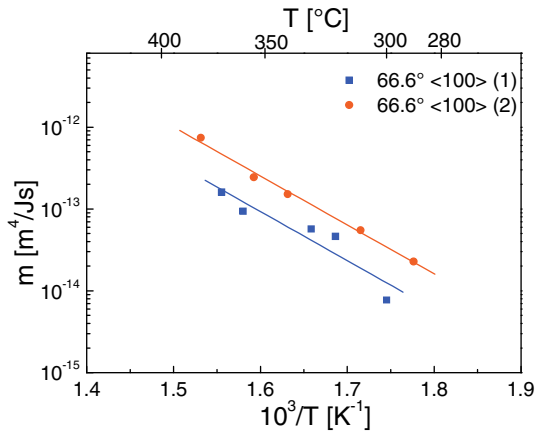


Fig. 10. Comparison of the mobility of a $66.6^\circ \langle 100 \rangle$ tilt boundary in bicrystals with different “second tilt” component $\xi_{66.6(1)} = 1.0^\circ$ and $\xi_{66.6(2)} = 2.1^\circ$ (Table 1).

is the case: the boundary mobility in bicrystals with the larger “second tilt” component was even higher than in the samples with lower “second tilt”. Similarly, the mobility of a $5.6^\circ \langle 100 \rangle$ boundary was found to be slightly higher than that of a $5.7^\circ \langle 100 \rangle$ boundary, although the “second tilt” component of the latter was smaller by a factor 2: $\xi_{5.6}/\xi_{5.7} = 2$ (Table 1). Second, if climb of dislocations which compensate the “second tilt” and “twist” angular deviations, i.e. atom diffusion across the boundary, controls boundary motion, the migration rate and migration activation parameters should be independent of the misorientation angle θ . However, as evident from Fig. 8, this is obviously not the case.

The activation enthalpies for stress-induced motion of high-angle boundaries with tilt angles close to low Σ CSL orientations were measured to be considerably lower than for low-angle and high-angle non-coincidence boundaries (Table 2, Fig. 8). Previously, when rationalizing why the migration activation enthalpy for high-angle boundaries was found to be smaller than for low-angle boundaries [23], it was suggested that the motion of high-angle boundaries is controlled by grain-boundary diffusion [44]. This interpretation, however, seems not to be applicable for the current results. The activation enthalpy for grain-boundary diffusion is known to be maximal for low Σ tilt boundaries and decreases with deviation from the coincidence misorientation [35,46]. The current measurements, however, revealed the opposite – for non-coincidence boundaries H was higher than for low Σ boundaries.

When comparing theoretical predictions and results of computer simulations with those of experimental measurements it is necessary to remember that materials considered in models and used in simulations are absolutely pure [8–13], whereas experiments are performed on bicrystals of a real material, i.e. in a material with impurities which tend to segregate to the grain boundary. As substantiated by the agreement between experimentally obtained and calculated coupling factors (Fig. 7), impurity segregation, which

may also alter the boundary structure compared to the structure of a model boundary, does not affect the geometric characteristics of the boundary migration mechanisms. On the other hand, it cannot be excluded that segregated impurity atoms and their motion together with the boundary may to a great extent affect the rate of stress-driven boundary migration. In fact, recent simulations by Elsener et al. [14] demonstrated that the presence of impurity atoms, particularly substitutional oxygen defects, can significantly affect the stress required for grain-boundary migration in Al.

4.4. Comparison with previous data on mechanically driven $\langle 100 \rangle$ tilt boundary motion in Al

In the past the migration of symmetrical tilt grain boundaries with various rotation axes ($\langle 112 \rangle$, $\langle 110 \rangle$ and $\langle 100 \rangle$) in Al bicrystals (99.99%) was studied by Fukutomi and co-workers [16–18,47]. Similarly, as in the current work, a constant stress creep device was used for tensile loading of bicrystals with grain boundaries tilted by 45° with respect to the applied stress. The applied tensile stresses were approximately in the same range as used in the current experiment. Unlike the current work though, the bicrystals were annealed under stress at much higher temperatures (between 400 and 550 °C) for very short time intervals up to 150 s.

Akin to the current results, the migration of the low-angle 4.5° , 7° and $10^\circ \langle 100 \rangle$ tilt boundaries in experiments by Fukutomi et al. was observed to be coupled to the shear strain of the sample defined by the misorientation angle of the boundary [47]. The migration activation enthalpy for a 4.5° boundary was obtained to be about 1.5 eV, in very good agreement with the current measurements (Fig. 8a). For $\langle 100 \rangle$ boundaries with $\theta = 7^\circ$ and $\theta = 10^\circ$, however, the values of H were about 0.9 eV. This decrease of the apparent migration activation enthalpy might be due to irregularities during boundary motion in the high-temperature regime with rising misorientation angle, such as alternate sliding events during boundary migration. In fact, a high-angle $\langle 100 \rangle$ boundary with $\theta = 22^\circ$ did not move at all, but demonstrated sliding along the boundary plane [47]. This is most probably due to the much higher temperature of annealing under stress than used in the current work.

The motion of $\langle 100 \rangle$ tilt grain boundaries in Al bicrystals was also reported by Winning [23–25]. The shear stress was used to cause boundary motion although, unlike the current experiments, the stress was a pure shear stress applied perpendicular to the boundary. The shear coupling was not investigated, however, and therefore a direct comparison of the results is not sensible.

5. Summary

The migration of planar grain boundaries in aluminum bicrystals under an applied constant external stress was investigated. Symmetrical low and high-angle $\langle 100 \rangle$ tilt

grain boundaries with rotation angles in the entire range between 0° and 90° were studied.

Shear stress-driven boundary migration was observed to be coupled to a lateral translation of the grains. Under the same applied external stress, boundaries with misorientations smaller than 31° and larger than 36° moved in opposite directions by two different mechanisms of this coupling. The measured ratios of normal boundary motion to the lateral displacement of grains are in an excellent agreement with theoretical predictions, i.e. they comply ideally with the respective boundary geometries.

Boundary migration was measured in the temperature range between 280 and 400 °C. From the temperature dependence of grain-boundary mobility the corresponding activation parameters (activation enthalpy H and mobility pre-exponential factor m_0) were determined. It was found that for mechanically induced grain-boundary motion there is a misorientation dependence of migration activation parameters. The lower H and m_0 values could be associated with the boundaries with misorientations close to low Σ CSL orientation relationships.

An analysis of the obtained activation parameters revealed that they comply with the compensation rule, i.e. there is a linear relationship between the activation enthalpy and the logarithm of the pre-exponential factor. As a consequence of the compensation effect, in the high-temperature regime the boundaries with higher activation enthalpy (low-angle and non-coincidence high-angle $\langle 100 \rangle$ tilt boundaries) moved faster, whereas at lower temperatures the boundaries with low activation enthalpy were more mobile.

Acknowledgements

The authors express their gratitude to the Deutsche Forschungsgemeinschaft for financial support (Grant MO 848/10-2). Helpful discussions with Professors Bevis Hutchinson and Lasar Shvindlerman are gratefully acknowledged.

References

- [1] Read WT, Shockley W. *Phys Rev* 1950;78:275.
- [2] Washburn J, Parker ER. *Trans AIME* 1952;194:1076.
- [3] Li CH, Edwards EH, Washburn J, Parker ER. *Acta Metall* 1953;1:223.
- [4] Bainbridge DW, Li CH, Edwards EH. *Acta Metall* 1954;2:322.
- [5] Peach M, Koehler JS. *Phys Rev* 1950;80:436.
- [6] Molodov DA, Ivanov VA, Gottstein G. *Acta Mater* 2007;55:1843.
- [7] Cahn JW, Taylor JE. *Acta Mater* 2004;52:4887.
- [8] Cahn JW, Mishin Y, Suzuki A. *Philos Mag* 2006;86:3965.
- [9] Cahn JW, Mishin Y, Suzuki A. *Acta Mater* 2006;54:4953.
- [10] Caillard D, Momprou F, Legros M. *Acta Mater* 2009;57:2390.
- [11] Suzuki A, Mishin Y. *Mater Sci Forum* 2005;502:157.
- [12] Ivanov VA, Mishin Y. *Phys Rev B* 2008;78:064106.
- [13] Zhang H, Du D, Srolovitz DJ. *Philos Mag* 2008;88:243.
- [14] Elsener A, Politano O, Derlet PM, Van Swygenhoven H. *Acta Mater* 2009;57:1988.
- [15] Watanabe T, Kimura SI, Karashima S. *Philos Mag A* 1984;49:845.
- [16] Horiuchi R, Fukutomi H, Takahashi T. In: Ishida Y, editor. *Fundamentals of diffusion bonding*. Amsterdam: Elsevier; 1987. p. 347.
- [17] Fukutomi H, Kamijo T. *Scr Metall* 1985;19:195.
- [18] Fukutomi H, Iseki T, Endo T, Kamijo T. *Acta Metall Mater* 1991;39:1445.
- [19] Sheikh-Ali AD, Valiev RZ. *Phys Status Solidi (a)* 1990;117:429.
- [20] Sheikh-Ali AD, Lavrentyev FF, Kazarov YuG. *Acta Mater* 1997;45:4505.
- [21] Sheikh-Ali AD, Szpunar JA. *Mater Sci Eng* 1998;A245:49.
- [22] Yoshida H, Yokoyama K, Shibata N, Ikuhara Y, Sakuma T. *Acta Mater* 2004;52:2349.
- [23] Winning M, Gottstein G, Shvindlerman LS. *Acta Mater* 2001;49:211.
- [24] Winning M. *Acta Mater* 2003;51:6465.
- [25] Winning M, Rollett AD. *Acta Mater* 2005;53:2109.
- [26] Momprou F, Caillard D, Legros M. *Acta Mater* 2009;57:2198.
- [27] Schiøtz J, Jacobsen KW. *Science* 2003;301:1357.
- [28] Meyers MA, Mishra A, Benson DJ. *Prog Mater Sci* 2006;51:427.
- [29] Haslam A, Moldovan D, Yamakov V, Wolf D, Phillpot S, Gleiter H. *Acta Mater* 2003;51:2112.
- [30] Farkas D, Frøseth A, Van Swygenhoven H. *Scr Mater* 2006;55:695.
- [31] Gianola GS, Van Petegem S, Legros M, Brandstetter S, Van Swygenhoven H, Hemker KJ. *Acta Mater* 2006;54:2253.
- [32] Legros M, Gianola GS, Hemker KJ. *Acta Mater* 2008;56:3380.
- [33] Sutton AP, Balluffi RW. *Interfaces in crystalline materials*. Oxford: Clarendon Press; 1995.
- [34] Molodov DA, Czubayko U, Gottstein G, Shvindlerman LS. *Acta Mater* 1998;46:553.
- [35] Surholt T, Molodov DA, Chr Herzig. *Acta Mater* 1998;46:5345.
- [36] Jiang WB, Kong QP, Molodov DA, Gottstein G. *Acta Mater* 2009;57:3327.
- [37] Peacock-López E, Suhl H. *Phys Rev B* 1982;26:3774.
- [38] Gottstein G, Shvindlerman LS. *Interface Sci* 1998;6:265.
- [39] Fridman EM, Kopecky ChV, Shvindlerman LS. *Z Metallkde* 1975;66:533.
- [40] Kirch DM. *In-situ SEM investigation of individual and connected grain boundaries in aluminum*. Göttingen: Cuvillier Verlag; 2008.
- [41] Kirch DM, Jannot E, Barrales-Mora LA, Molodov DA, Gottstein G. *Acta Mater* 2008;56:4998.
- [42] Hirth JP, Pond RC, Lothe J. *Acta Mater* 2006;54:4237.
- [43] Smithells CJ. *Smithells reference book*. London: Butterworth; 1983.
- [44] Winning M, Gottstein G, Shvindlerman LS. *Acta Mater* 2002;50:353.
- [45] Molodov DA, Gorkaya T, Gottstein G. *Mater Sci Forum* 2007;558–559:927.
- [46] Aleshin AN, Bokstein BS, Shvindlerman LS. *Sov Phys Chem Mech Surf* 1982;6:1.
- [47] Fukutomi H, Horiuchi R. *Trans Jap Inst Met* 1981;22:633.